Progress of Theoretical Physics, Vol. 105, No. 6, June 2001

Structure of Chiral Phase Transitions at Finite Temperature in Abelian Gauge Theories

Kenji Fukazawa, Tomohiro Inagaki,* Seiji Mukaigawa** and Taizo Muta***

Kure National College of Technology, Kure 737-8506, Japan
**Information Media Center, Hiroshima University, Higashi-Hiroshima 739-8521 Japan*
***Department of Electrical and Electronic Engineering, Faculty of Engineering Iwate University, Morioka 020-8551, Japan*
****Department of Physics, Hiroshima University, Higashi-Hiroshima 739-8526 Japan*

(Received June 27, 2000)

The mechanism of chiral symmetry breaking is investigated in strong-coupling Abelian gauge theories at finite temperature. The Schwinger-Dyson equation in the Landau gauge is employed in the real time formalism and is solved numerically within the framework of the instantaneous exchange approximation, including the effect of the thermal mass for the photon propagator. It is found that the chiral symmetry is broken below the critical temperature T for sufficiently large coupling α. The chiral phase transition is found to be of second order, and the phase diagram in the T-α plane is obtained. It is investigated how the structure of the chiral phase transition is affected by the thermal mass in the photon propagator.

§1. Introduction

The chiral phase transition in gauge field theories at finite temperature is an interesting phenomenon in many respects. In particular, it plays an important role when we deal with the early stage of the universe. It has been known for a long time that Abelian gauge theories at vanishing temperature are subject to chiral symmetry breaking in the strong coupling region, and hence the massless fermions acquire a mass in a dynamical way.[1)-4)] This phenomenon has been studied mostly by using the Schwinger-Dyson equation.[5)]

It is quite natural from the point of view of the early universe to introduce a temperature effect in the analysis of the above phenomenon. Then, it is interesting to determine whether the broken chiral symmetry at vanishing temperature is restored at sufficiently high temperature and examine whether the phase transition is of first order or second order. There have been several works dealing with this problem in quantum chromodynamics. There have, however, not been many works[6)-8)] which have studied this question by taking into account the fermion wave function effect and the thermal photon mass. For this reason, we attempt to carry out a thorough analysis of the chiral phase transition in Abelian gauge theories at finite temperature with due consideration of the thermal photon mass by using the Schwinger-Dyson equation.

In our analysis we use the Schwinger-Dyson equation in the real time formalism

to introduce the temperature.[9)-12)] To solve the Schwinger-Dyson equation we confine ourselves to the instantaneous exchange approximation. This approximation is found to be valid in the high temperature region. In the case of vanishing temperature, the vacuum polarization effect is negligible. For high temperature, the vacuum polarization becomes enhanced, and so within our approximation we are forced to take into account the vacuum polarization function in the photon propagator while dealing with the Schwinger-Dyson equation.

Our analysis of the finite-temperature Schwinger-Dyson equation consists mostly of numerical calculations. We find that our numerical solutions are quite stable, and the results are proven to be reliable. From the numerical analysis we recognize that the fermion wave function effect is negligible at high temperature. We observe a clear signal of a second order chiral phase transition as temperature varies. We investigate the thermal photon mass effect in the chiral phase transition. We obtain critical curves in the T-α plane, with T the temperature and α the fine structure constant.

§2. Schwinger-Dyson equation at finite temperature

Throughout this paper we use Abelian gauge theories, in particular, quantum electrodynamics with massless fermions. The main purpose of our work is to see whether the broken chiral symmetry for large α at vanishing temperature is restored at high temperature and, if so, to determine the nature of the chiral phase transition, i.e., whether it is first order or second order. Here α is the fine structure constant, $\alpha = e^2/4\pi$, with e the electric charge of fermions. We rely on the Schwinger-Dyson equation in the real time formalism of the finite-temperature field theory. In the imaginary time approach, the integral equation is cast into an infinite-component simultaneous equation, including infinite sums, and it is very hard to handle this summation properly.

We start with a brief summary of the Schwinger-Dyson equation for vanishing temperature, $T = 0$. The Schwinger-Dyson equation for the fermion self-energy part $\Sigma(p)$ reads, within the ladder approximation in the Landau gauge,

$$\Sigma(p) = -ie^2 \int \frac{d^4q}{(2\pi)^4} \gamma^\mu iS(q) \gamma^\nu iD^{\rm tree}_{\mu\nu}(p-q), \tag{2·1}$$

where $D^{\rm tree}_{\mu\nu}(p-q)$ is the photon propagator at the tree level, and the self-energy part $\Sigma(p)$ is defined through

$$iS(p) = \frac{i}{\not p - \Sigma(p) + i\varepsilon} = \frac{i}{A(p^2)\not p - B(p^2) + i\varepsilon}, \tag{2·2}$$

with $S(p)$ the full propagator for massless fermions, and $A(p^2)$ and $B(p^2)$ invariant functions of p^2. By use of the invariant functions, the self-energy part can be written such that $\Sigma(p) = (1 - A(p^2))\not p + B(p^2)$. It has been known for a long time[1)-3)] that Eq. (2·1) possesses a non-vanishing solution for $B(p^2)$ with $A(p^2) = 1$ if $\alpha > \alpha_c = \pi/3$. Thus chiral symmetry is broken for unusually large electromagnetic couplings, and the massless fermion acquires a dynamical mass for $\alpha > \pi/3$.

At finite temperature in the real time formalism,[9)-12)] the full propagator for fermions may be written in the following form:

$$iS(p) = \frac{i}{\not{p} - \Sigma(p) + i\varepsilon} = \frac{i}{A_0(p_0, |\vec{p}|)p_0\gamma^0 + A(p_0, |\vec{p}|)p_i\gamma^i - B(p_0, |\vec{p}|) + i\varepsilon}. \quad (2\cdot3)$$

In the closed time path method,[12)] the spinor self-energy part is given by the matrix form

$$i\Sigma^{ab}(p) = V^{-1}(\beta, p)\begin{pmatrix} i\Sigma(p) & 0 \\ 0 & -i\Sigma^*(p) \end{pmatrix} V^{-1}(\beta, p), \quad (2\cdot4)$$

where $V(\beta, p)$ is the unitary matrix that connects the thermal vacuum to the zero-temperature vacuum, and is given by

$$V(\beta, p) = \begin{pmatrix} \cos\varphi & -\epsilon(p_0)\sin\varphi \\ \epsilon(p_0)\sin\varphi & \cos\varphi \end{pmatrix}, \quad (2\cdot5)$$

with

$$\cos\varphi = \frac{1}{\sqrt{1+\exp(-\beta|p_0|)}}; \quad \sin\varphi = \frac{\exp(-\beta|p_0|/2)}{\sqrt{1+\exp(-\beta|p_0|)}}. \quad (2\cdot6)$$

Accordingly, we find

$$\begin{aligned} \Sigma^{11}(p) &= \not{p} - \mathrm{Re}A_0(p_0, |\vec{p}|)p_0\gamma^0 - \mathrm{Re}A(p_0, |\vec{p}|)p_i\gamma^i + \mathrm{Re}B(p_0, |\vec{p}|) \\ &-i[\mathrm{Im}A_0(p_0, |\vec{p}|)p_0\gamma^0 - \mathrm{Im}A(p_0, |\vec{p}|)p_i\gamma^i + \mathrm{Im}B(p_0, |\vec{p}|)]\tanh\frac{\beta|p_0|}{2}, \end{aligned} \quad (2\cdot7)$$

and hence

$$\begin{aligned} &\mathrm{Re}A_0(p_0, |\vec{p}|)p^0 = p^0 - \frac{1}{\mathrm{tr}1}\mathrm{tr}[\gamma^0\mathrm{Re}\Sigma^{11}], \\ &\mathrm{Im}A_0(p_0, |\vec{p}|)p^0\tanh\frac{\beta|p_0|}{2} = -\frac{1}{\mathrm{tr}1}\mathrm{tr}[\gamma^0\mathrm{Im}\Sigma^{11}], \\ &\mathrm{Re}A(p_0, |\vec{p}|)p^i = p^i - \frac{1}{\mathrm{tr}1}\mathrm{tr}[\gamma^i\mathrm{Re}\Sigma^{11}], \\ &\mathrm{Im}A(p_0, |\vec{p}|)p^i\tanh\frac{\beta|p_0|}{2} = -\frac{1}{\mathrm{tr}1}\mathrm{tr}[\gamma^i\mathrm{Im}\Sigma^{11}], \\ &\mathrm{Re}B(p_0, |\vec{p}|) = \frac{1}{\mathrm{tr}1}\mathrm{tr}[\mathrm{Re}\Sigma^{11}], \\ &\mathrm{Im}B(p_0, |\vec{p}|)\tanh\frac{\beta|p_0|}{2} = \frac{1}{\mathrm{tr}1}\mathrm{tr}[\mathrm{Im}\Sigma^{11}], \end{aligned} \quad (2\cdot8)$$

The Schwinger-Dyson equation in the real time formalism is written in matrix form within the framework of the closed time path method. If the vertex part is approximated by a tree form, the 1-1 matrix element of the equation can be represented by only the 1-1 component of the fermion and photon propagator and takes the form

$$\Sigma^{11}(p) = -ie^2\int\frac{d^4q}{(2\pi)^4}\gamma^\mu iS^{11}(q)\gamma^\nu iD^{11}_{\mu\nu}(p-q). \quad (2\cdot9)$$

Here, the spinor two-point function $S^{11}(p)$ is given by evaluating the 1-1 matrix element of the expression [6), 7)]

$$iS^{ab}(p) = V(\beta,p)\begin{pmatrix} S(p) & 0 \\ 0 & S^*(p) \end{pmatrix} V(\beta,p), \tag{2·10}$$

and reads

$$\begin{aligned} iS^{11}(p) = &\frac{i}{\not p - \Sigma(p) + i\varepsilon} \\ &- \left[\frac{i}{\not p - \Sigma(p) + i\varepsilon} - \frac{i}{\not p - \Sigma^*(p) - i\varepsilon}\right] \times \frac{1}{e^{\beta|p_0|}+1}. \end{aligned} \tag{2·11}$$

The photon two-point function $D^{11}_{\mu\nu}(p)$ is also found by evaluating the 1-1 matrix element of the matrix

$$iD^{ab}_{\beta}(q) = U(\beta,q)\begin{pmatrix} D_{\mu\nu}(q) & 0 \\ 0 & D^*_{\mu\nu}(q) \end{pmatrix} U(\beta,q), \tag{2·12}$$

where

$$U(\beta,q) = \begin{pmatrix} \cosh\theta & \sinh\theta \\ \sinh\theta & \cosh\theta \end{pmatrix}, \tag{2·13}$$

$$\cosh\theta = \frac{1}{\sqrt{1-\exp(-\beta|q_0|)}}; \quad \sinh\theta = \frac{\exp(-\beta|q_0|/2)}{\sqrt{1-\exp(-\beta|q_0|)}}. \tag{2·14}$$

The general form of the photon propagator at finite temperature is well known and is given by [11)]

$$iD_{\mu\nu}(q) = \frac{i}{q^2 - \Pi^T(q) + i\varepsilon}P^T_{\mu\nu}(q) + \frac{i}{q^2 - \Pi^L(q) + i\varepsilon}P^L_{\mu\nu}(q) - i\frac{\alpha_{\rm GF}}{q^2+i\varepsilon}\frac{q_\mu q_\nu}{q^2}, \tag{2·15}$$

where $P^T_{\mu\nu}(q)$ and $P^L_{\mu\nu}(q)$ are the transverse and longitudinal projection operators, and $\alpha_{\rm GF}$ is the gauge fixing parameter. Below we use the Landau gauge, $\alpha_{\rm GF}=0$, which is consistent with the Ward-Takahashi identity within the ladder approximation at $T=0$.*) We then find that

$$iD^{11}_{\mu\nu}(q) = {\rm Re}iD_{\mu\nu}(q)\coth\frac{\beta|q_0|}{2} + i{\rm Im}iD_{\mu\nu}(q). \tag{2·16}$$

Below we adopt the instantaneous exchange approximation for the photon propagator (2·16) and solve the Schwinger-Dyson equation (2·9).

§3. Instantaneous exchange approximation

In order to derive as much information regarding the phase structure of quantum electrodynamics at finite temperature as possible, we attempt to solve the

*) At finite temperature, the Ward-Takahashi identity is not guaranteed within the ladder approximation in the Landau gauge. In §4, we see that the fermion wave functions A_0 and A are almost unity, and the Ward-Takahashi identity nearly holds at high temperature.

Schwinger-Dyson equation describing it as an integral equation for the functions $A_0(p_0, |\vec{p}|), A(p_0, |\vec{p}|)$ and $B(p_0, |\vec{p}|)$. To solve the equation, it is necessary to make some approximation which may not have any serious influence on the resulting physical predictions. Throughout the paper we apply the instantaneous exchange approximation. In the imaginary-time formalism, the term that contains $\coth(\beta|\mathrm{q}_0|/2)$ is generated by a summation over Matsubara frequencies. In addition, we assume that the higher frequency modes are decoupled, and we neglect the term proportional to $\coth(\beta|\mathrm{q}_0|/2)$ in the photon propagator. The approximation implies that the vacuum polarization function is real and independent of q_0. The instantaneous exchange approximation is believed to be valid at high temperature $(4\pi^2T^2 \gg \vec{q}^2 + \Pi^{T,L}(q))$.[7] Since we consider the strong coupling theory, it is necessary to solve the simultaneous Schwinger-Dyson equation for fermion and photon propagators. However, the thermal part of the vacuum polarization function is expected to be proportional to T^2. As the functional form of the vacuum polarization function, we adopt [*]

$$\Pi^T(q_0, q)|_{q_0\to 0} \sim 0, \qquad \Pi^L(q_0, q)|_{q_0\to 0} \sim 2Nm_{\mathrm{ph}}^2 \equiv Ng(e)\frac{e^2}{3}T^2, \tag{3·1}$$

where N is the number of fermion flavors and $g(e)$ is a function of the coupling constant e. We regard $Ng(e)$ as a parameter and solve the Schwinger-Dyson equation for the fermion propagator below.

In the manner described above, we obtain

$$iD^{11}_{\mu\nu}(q) = -\mathcal{P}\frac{i}{\vec{q}^2}P^T_{\mu\nu}(q) - \mathcal{P}\frac{i}{\vec{q}^2 + 2Nm_{\mathrm{ph}}^2}P^L_{\mu\nu}(q), \tag{3·2}$$

where $P^T_{\mu\nu}(q)$ and $P^L_{\mu\nu}(q)$ are described in the instantaneous exchange approximation as

$$P^T_{0\mu}(q) = 0,\ P^T_{ij}(q) = \delta_{ij} - \frac{q_iq_j}{\vec{q}^2}, \tag{3·3}$$

$$P^L_{\mu\nu}(q) = \begin{cases} -1 & \mu = \nu = 0, \\ 0 & \text{others.} \end{cases} \tag{3·4}$$

With this approximation, the Schwinger-Dyson equation is rewritten as

$$\begin{aligned}\Sigma^{11}(p) &= -ie^2\int\frac{d^4q}{(2\pi)^4}\gamma^\mu iS^{11}(q)\gamma^\nu iD^{11}_{\mu\nu}(\vec{p}-\vec{q}) \\ &= (1-\mathrm{Re}A_0(p_0,|\vec{p}|))p_0\gamma^0 + (1-\mathrm{Re}A(p_0,|\vec{p}|))p_i\gamma^i + \mathrm{Re}B(p_0,|\vec{p}|) \\ &\quad -i(\mathrm{Im}A_0(p_0,|\vec{p}|)p_0\gamma^0 + \mathrm{Im}A(p_0,|\vec{p}|)p_i\gamma^i - \mathrm{Im}B(p_0,|\vec{p}|))\tanh\frac{\beta|p_0|}{2}.\end{aligned} \tag{3·5}$$

Since the right-hand side of the first line in Eq. (3·5) has no p_0 dependence in this approximation, the fermion self-energy Σ^{11} is independent of p_0, and thus the

[*] We neglect the photon damping constant, which disappears in the static limit.

functions $A_0(p_0,|\vec{p}|)$, $A(p_0,|\vec{p}|)$ and $B(p_0,|\vec{p}|)$ can be written as

$$\begin{aligned}
c_r(|\vec{p}|) &\equiv (1-\mathrm{Re}A_0(p_0,|\vec{p}|))p_0,\\
A_r(|\vec{p}|) &\equiv \mathrm{Re}A(p_0,|\vec{p}|),\\
B_r(|\vec{p}|) &\equiv \mathrm{Re}B(p_0,|\vec{p}|),\\
c_i(|\vec{p}|) &\equiv -\mathrm{Im}A_0(p_0,|\vec{p}|)p_0\tanh\frac{\beta|p_0|}{2},\\
a_i(|\vec{p}|) &\equiv -\mathrm{Im}A(p_0,|\vec{p}|)\tanh\frac{\beta|p_0|}{2}\\
b_i(|\vec{p}|) &\equiv \mathrm{Im}B(p_0,|\vec{p}|)\tanh\frac{\beta|p_0|}{2}
\end{aligned} \tag{3·6}$$

respectively.

Substituting Eqs. (2·11) and (3·2) into Eq. (3·5), we obtain the Schwinger-Dyson equation in our approximation. If any one of A_0, A or B has a non-vanishing imaginary part, we obtain in the following simultaneous equations:

$$\begin{aligned}
c_r(|\vec{p}|) = &-\frac{\alpha}{4\pi^2|\vec{p}|}\int_{-\Lambda}^{\Lambda}dq^0\int_0^{\Lambda}d|\vec{q}||\vec{q}|\left[-2\ln\left(\frac{|\vec{p}|+|\vec{q}|}{|\vec{p}|-|\vec{q}|}\right)^2+\ln\frac{(|\vec{p}|+|\vec{q}|)^2+2Nm_{\mathrm{ph}}^2}{(|\vec{p}|-|\vec{q}|)^2+2Nm_{\mathrm{ph}}^2}\right]\\
&\times\left[-c_i(|\vec{q}|)\mathrm{Re}f(q)+(q^0-c_r(|\vec{q}|))\mathrm{Im}f(q)\tanh\frac{\beta|q_0|}{2}\right],
\end{aligned} \tag{3·7}$$

$$\begin{aligned}
c_i(|\vec{p}|) = &\frac{\alpha}{4\pi^2|\vec{p}|}\int_{-\Lambda}^{\Lambda}dq^0\int_0^{\Lambda}d|\vec{q}||\vec{q}|\left[-2\ln\left(\frac{|\vec{p}|+|\vec{q}|}{|\vec{p}|-|\vec{q}|}\right)^2+\ln\frac{(|\vec{p}|+|\vec{q}|)^2+2Nm_{\mathrm{ph}}^2}{(|\vec{p}|-|\vec{q}|)^2+2Nm_{\mathrm{ph}}^2}\right]\\
&\times\left[-(q^0-c_r(|\vec{q}|))\mathrm{Re}f(q)+c_i(|\vec{q}|)\mathrm{Im}f(q)\tanh^{-1}\frac{\beta|q_0|}{2}\right],
\end{aligned} \tag{3·8}$$

$$\begin{aligned}
(A_r(|\vec{p}|)-1)|\vec{p}|^2 = &-\frac{\alpha}{8\pi^2|\vec{p}|}\int_{-\Lambda}^{\Lambda}dq^0\int_0^{\Lambda}d|\vec{q}||\vec{q}|\\
&\times\left[(|\vec{p}|^2+|\vec{q}|^2+2Nm_{\mathrm{ph}}^2)\ln\frac{(|\vec{p}|+|\vec{q}|)^2+2Nm_{\mathrm{ph}}^2}{(|\vec{p}|-|\vec{q}|)^2+2Nm_{\mathrm{ph}}^2}-4|\vec{p}||\vec{q}|\right]\\
&\times\left[-a_i(|\vec{q}|)\mathrm{Re}f(q)+A_r(|\vec{q}|)\mathrm{Im}f(q)\tanh\frac{\beta|q_0|}{2}\right],
\end{aligned} \tag{3·9}$$

$$\begin{aligned}
a_i(|\vec{p}|)|\vec{p}|^2 = &-\frac{\alpha}{8\pi^2|\vec{p}|}\int_{-\Lambda}^{\Lambda}dq^0\int_0^{\Lambda}d|\vec{q}||\vec{q}|\\
&\times\left[(|\vec{p}|^2+|\vec{q}|^2+2Nm_{\mathrm{ph}}^2)\ln\frac{(|\vec{p}|+|\vec{q}|)^2+2Nm_{\mathrm{ph}}^2}{(|\vec{p}|-|\vec{q}|)^2+2Nm_{\mathrm{ph}}^2}-4|\vec{p}||\vec{q}|\right]\\
&\times\left[-A_r(|\vec{q}|)\mathrm{Re}f(q)+a_i(|\vec{q}|)\mathrm{Im}f(q)\tanh^{-1}\frac{\beta|q_0|}{2}\right],
\end{aligned} \tag{3·10}$$

$$B_r(|\vec{p}|) = \frac{\alpha}{4\pi^2|\vec{p}|}\int_{-\Lambda}^{\Lambda} dq^0 \int_0^{\Lambda} d|\vec{q}||\vec{q}| \left[2\ln\left(\frac{|\vec{p}|+|\vec{q}|}{|\vec{p}|-|\vec{q}|}\right)^2 + \ln\frac{(|\vec{p}|+|\vec{q}|)^2+2Nm_{\rm ph}^2}{(|\vec{p}|-|\vec{q}|)^2+2Nm_{\rm ph}^2}\right]$$
$$\times\left[b_i(|\vec{q}|){\rm Re}f(q) + B_r(|\vec{q}|){\rm Im}f(q)\tanh\frac{\beta|q_0|}{2}\right], \tag{3·11}$$

$$b_i(|\vec{p}|) = \frac{\alpha}{4\pi^2|\vec{p}|}\int_{-\Lambda}^{\Lambda} dq^0 \int_0^{\Lambda} d|\vec{q}||\vec{q}| \left[2\ln\left(\frac{|\vec{p}|+|\vec{q}|}{|\vec{p}|-|\vec{q}|}\right)^2 + \ln\frac{(|\vec{p}|+|\vec{q}|)^2+2Nm_{\rm ph}^2}{(|\vec{p}|-|\vec{q}|)^2+2Nm_{\rm ph}^2}\right]$$
$$\times\left[B_r(|\vec{q}|){\rm Re}f(q) - b_i(|\vec{q}|){\rm Im}f(q)\tanh^{-1}\frac{\beta|q_0|}{2}\right], \tag{3·12}$$

where

$$f(q) = \frac{1}{A_0^2q_0^2 - A^2|\vec{q}|^2 - B^2}. \tag{3·13}$$

To regularize the integral, the cutoff scale Λ is introduced. Then to see if the fermion acquires a dynamical mass or not, we study the chiral phase transition in terms of bare quantities. If A_0, A and B each has no imaginary part, the Schwinger-Dyson equation reduces to the following simultaneous equations:

$$c_r(p) = \frac{\alpha}{8\pi p}\int_0^{\Lambda} dqq\left(\tanh\frac{\beta|c_r(q)+\omega_q|}{2} - \tanh\frac{\beta|c_r(q)-\omega_q|}{2}\right)$$
$$\times\left[-2\ln\left(\frac{p+q}{p-q}\right)^2 + \ln\frac{(p+q)^2+2Nm_{\rm ph}^2}{(p-q)^2+2Nm_{\rm ph}^2}\right], \tag{3·14}$$

$$(A(p)-1)p^2 = \frac{\alpha}{16\pi p}\int_0^{\Lambda} dq\frac{qA(q)}{\omega_q}\left(\tanh\frac{\beta|c_r(q)+\omega_q|}{2} + \tanh\frac{\beta|c_r(q)-\omega_q|}{2}\right)$$
$$\times\left[(p^2+q^2+2Nm_{\rm ph}^2)\ln\frac{(p+q)^2+2Nm_{\rm ph}^2}{(p-q)^2+2Nm_{\rm ph}^2} - 4pq\right], \tag{3·15}$$

$$B(p) = \frac{\alpha}{8\pi p}\int_0^{\Lambda} dq\frac{qB(q)}{\omega_q}\left(\tanh\frac{\beta|c_r(q)+\omega_q|}{2} + \tanh\frac{\beta|c_r(q)-\omega_q|}{2}\right)$$
$$\times\left[2\ln\left(\frac{p+q}{p-q}\right)^2 + \ln\frac{(p+q)^2+2Nm_{\rm ph}^2}{(p-q)^2+2Nm_{\rm ph}^2}\right], \tag{3·16}$$

where we set $p = |\vec{p}|$ and $q = |\vec{q}|$ and $\omega_q \equiv \sqrt{A^2(q)q^2 + B^2(q)}$. In the following sections, we report the numerical analysis of the Schwinger-Dyson equation and study the behavior of the mass function $B(p)$ to derive information on the phase transitions.

§4. Numerical solutions

The task under consideration is solving Eqs. (3·7)–(3·12) or (3·14)–(3·16) numerically. There are several different numerical methods available for solving integral

equations like (3·7)–(3·12) or (3·14)–(3·16). Among these, there exist two standard methods. One consists of discretizing the integral in Eqs. (3·7)–(3·12) or (3·14)–(3·16) and regarding the resulting equations as simultaneous equations. The other standard method consists of starting with suitable trial functions for the solution and iterating the calculational procedure until stable solutions are obtained. It seems that the latter method is much simpler to handle and is useful as long as the convergence of the iteration is guaranteed. We employed the latter method in our analysis.

We begin with the simplest possible choice for the trial functions in the iteration. Thus the trial functions are chosen to be constants, independent of p:

$$c(p) = \text{constant}, \quad A(p) = \text{constant}, \quad B(p) = \text{constant}. \tag{4·1}$$

At each iteration, the integration is performed by using the Monte Carlo method, and the integral is cut off at mass scale Λ. After the first iteration, the resulting mass function acquires a p dependence, and it is substituted into the mass function in the integral on the right-hand sides of Eqs. (3·7)–(3·12) or (3·14)–(3·16). Repeating this procedure, we may obtain a stable result. Whether we have a stable result or not should be always checked after sufficiently many iterations. In each calculation, we confirmed the stability of the solution.

We first consider the case with non-vanishing imaginary part for at least one of A_0, A or B and solve the simultaneous equations (3·7)–(3·12) with this iteration procedure. After some numerical calculations, it was found that the solution is not stable or that A_0, A and B approach purely real values at each iteration. In other words, we cannot find any stable solution with non-vanishing imaginary part for Eqs. (3·7)–(3·12).

We next consider the real solution for A_0, A and B. To obtain a real solution we solved the simultaneous equations (3·14)–(3·16) with thermal photon mass $Ng = 1$. Note here that the parameter Ng plays the role of switching on ($Ng = 1$) and off ($Ng = 0$) the photon mass, and also represents the number of fermion flavors. In Eq. (3·14) we easily see that $c_r(p) = 0$ if $c_r(p)$ is positive definite or negative definite. We examine whether the result is correct for a wider class of trial functions for $c_r(p)$, i.e., we started from some suitable alternating trial functions for $c_r(p)$ and obtained the result $c_r(p) = 0$.

In Fig. 1, the function $B(p)$ normalized by the cutoff Λ of the p integration is presented as a function of the number of iterations for the case with $p = 0.1\Lambda$ and $T = 0.01\Lambda$, 0.10Λ, 0.14Λ. Here, we adopt units for which $k = 1$, where k is the Boltzmann constant. The fluctuations observed in Fig. 1 arise from errors in the Monte Carlo integration. As seen in Fig. 1, the resulting function becomes stable after about 100 iterations. The function $A(p)$ behaves essentially in the same way as $B(p)$ and it becomes stable after about 100 iterations. We then continued our analysis by taking many more points for the values of the momentum and obtained the momentum dependence of the solution of the Schwinger-Dyson equation. In Figs. 2 and 3 the functions $A(p)$ and $B(p)/\Lambda$ are presented as functions of the momentum p normalized by the cutoff. The functions presented there were obtained after 1200 iterations. As is seen in Figs. 2 and 3, $A(p)$ and $B(p)$ are smooth functions of p, and the momentum dependence of $A(p)$ and $B(p)$ is not too strong. Hence,

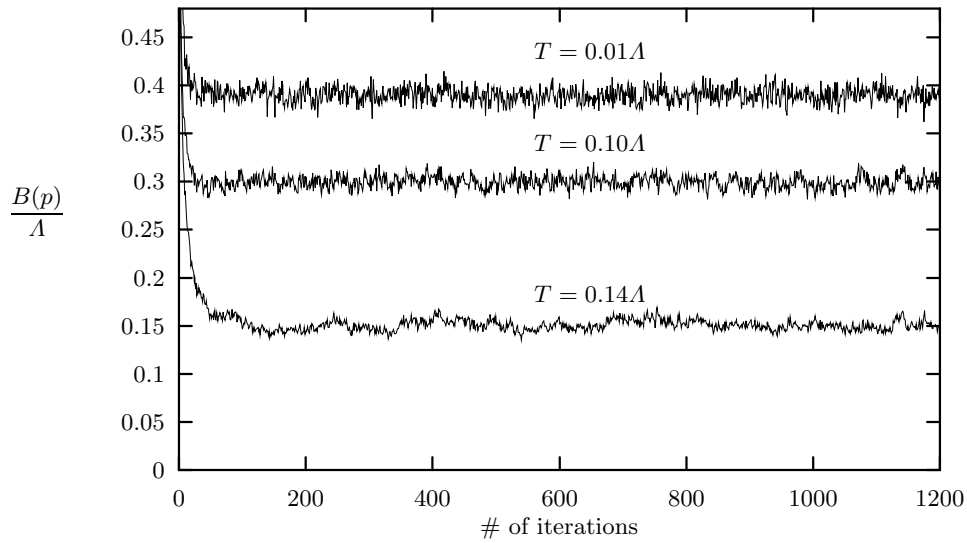

Fig. 1. Typical behavior of a solution of the Schwinger-Dyson equation (3·16) for $Ng = 1$, $\alpha = 1$, and $p = 0.1\Lambda$.

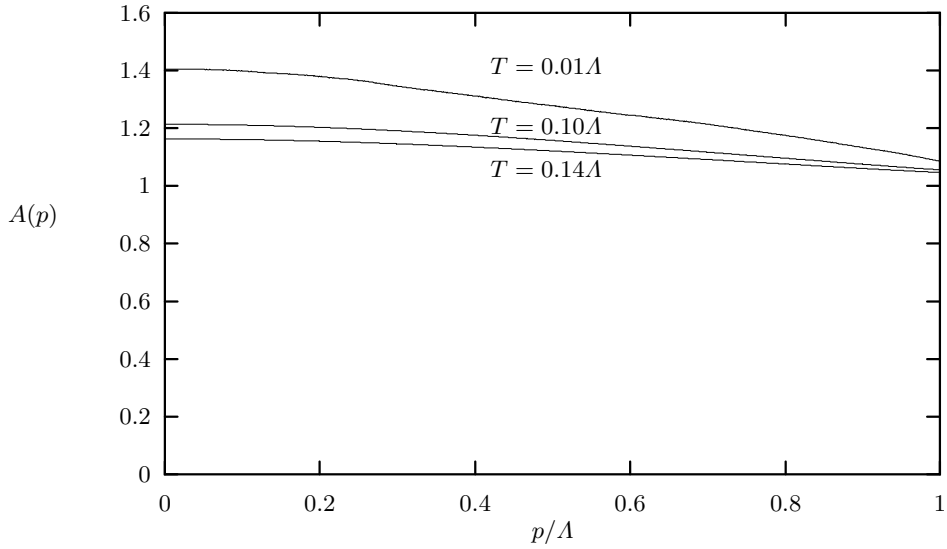

Fig. 2. Typical shape of the function $A(p)$ for $Ng = 1$ and $\alpha = 1$.

we use $B(p = 0.1\Lambda)$ as the order parameter of the chiral symmetry breaking instead of the value at $p = 0$, where the IE approximation may be valid for smaller T. It should be noted here that the convergence of the iterations for $B(p)$ becomes slower near the critical value of the coupling constant α and temperature T. In this case, we need more iterations to obtain a stable result for the mass function $B(p)$.

The case without a thermal photon mass, $Ng = 0$, is studied essentially in the

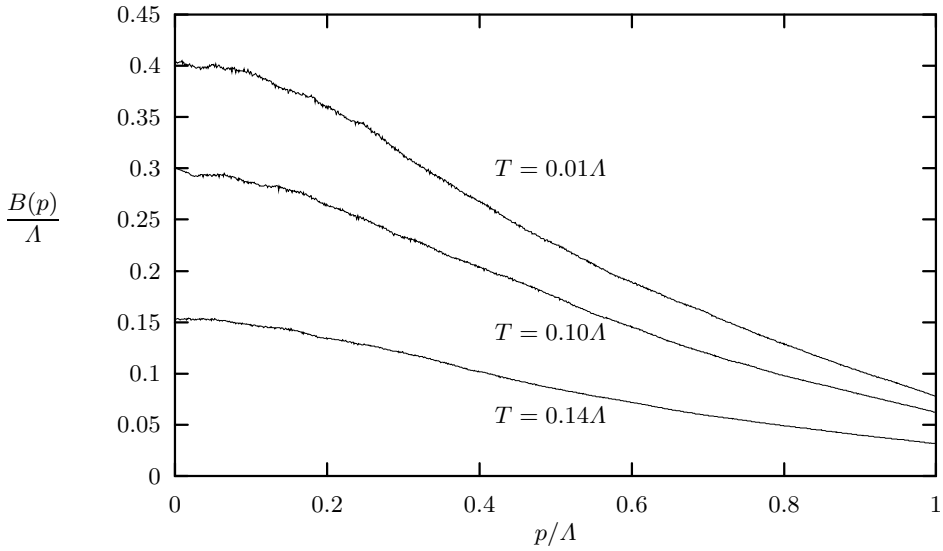

Fig. 3. Typical shape of the mass function $B(p)$ for $Ng = 1$ and $\alpha = 1$.

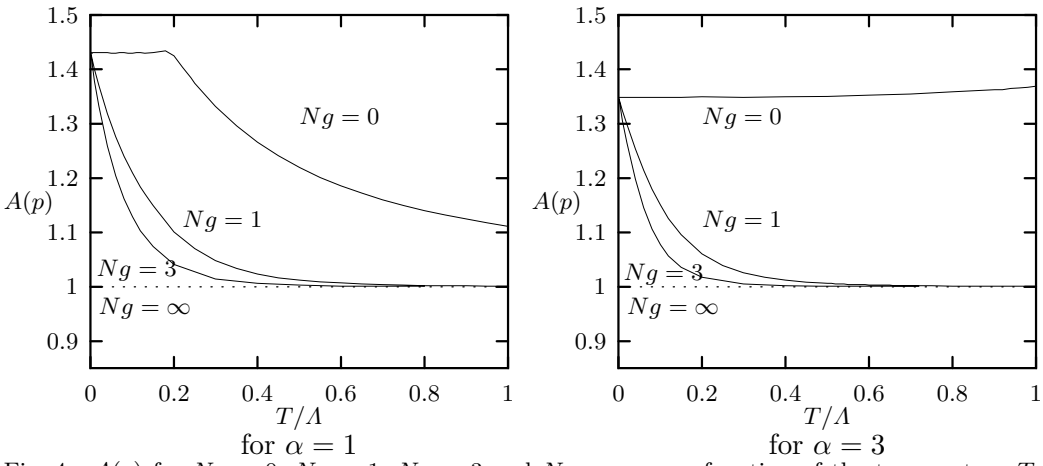

Fig. 4. $A(p)$ for $Ng = 0$, $Ng = 1$, $Ng = 3$ and $Ng = \infty$ as a function of the temperature T at $p = 0.1$.

same manner as described above. We may also study the case with three fermion flavors $Ng = 3$ essentially in the same manner. Here we skip to present the numerical results on the mass function.

In Fig. 4 the T dependence of $A(p)$ is presented. We observe that $A(p)$ is almost unity for high temperature, except in the case $Ng = 0$.

We conclude in this section that $A_0(p) = 1$ $[c_r(p) = 0]$ and $A(p) = 1$ for sufficiently high temperature. Accordingly, in the following sections we study the possible chiral phase transition by considering numerical investigation only of the mass func-

tion $B(p)$. In the case $Ng = 0$, it is not difficult to show that the conclusions are not affected by the deviation of $A(p)$ from unity.

§5. Chiral phase transitions

We first wish to observe the behavior of the mass function at some fixed value of p as a function of the parameters α and T. The α dependence of the mass function $B(p)$ with $p = 0.1\Lambda$ is shown in Fig. 5 for various fixed values of T. Note here that the errors resulting from the fluctuations observed in Fig. 1 are smaller than the size of the symbol used for each sample point in Fig. 5.

As is clearly seen in Fig. 5, the chiral phase transition is of second order, since a fermion mass is generated at a critical value of the coupling constant α without any discontinuity. By picking up the critical value of α, where the mass generation occurs, one can obtain the critical parameters α_c and T_c. If T_c is plotted versus α_c, we obtain the phase diagram. We will come back to this subject in §6. It should be noted here that the value of the critical coupling constant α_c for $T = 0$ is found to be 0.44477 ± 0.00053 (see Appendix A). This value differs from the well-known value $\pi/3$. The reason for this is simple: In our approach we applied the instantaneous exchange approximation, which is not a good approximation in the low temperature region. Thus we have to be careful in applying our method and consider our formulation to be suitable rather in the high temperature region.

We can also observe the behavior of the mass function $B(p)$ at some fixed value of p as a function of temperature T. The T dependence of $B(p)$ with $p = 0.1\Lambda$ is given in Fig. 6 for fixed α. Here, again, we clearly observe the second order chiral phase transition in Fig. 6.

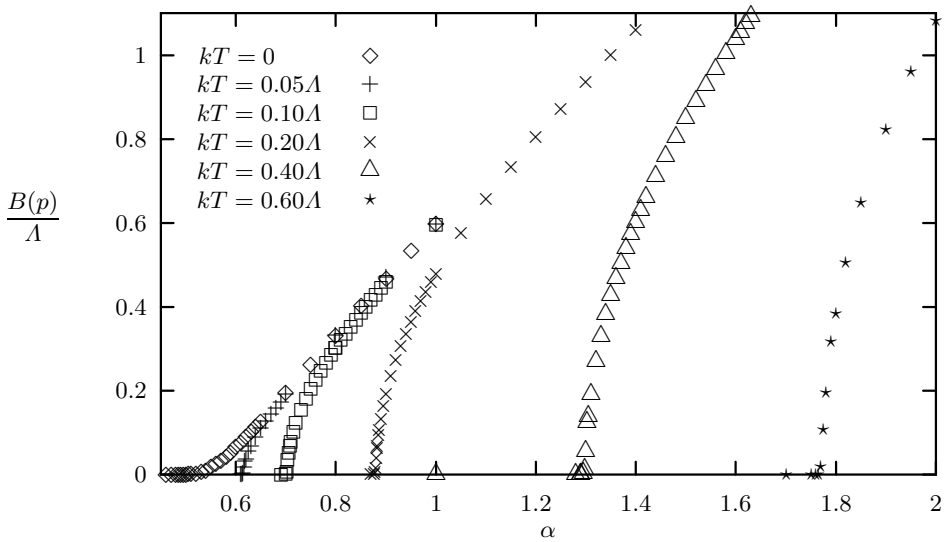

Fig. 5. Dynamical fermion mass as a function of the coupling constant α for $Ng = 0$ at $p = 0.1\Lambda$.

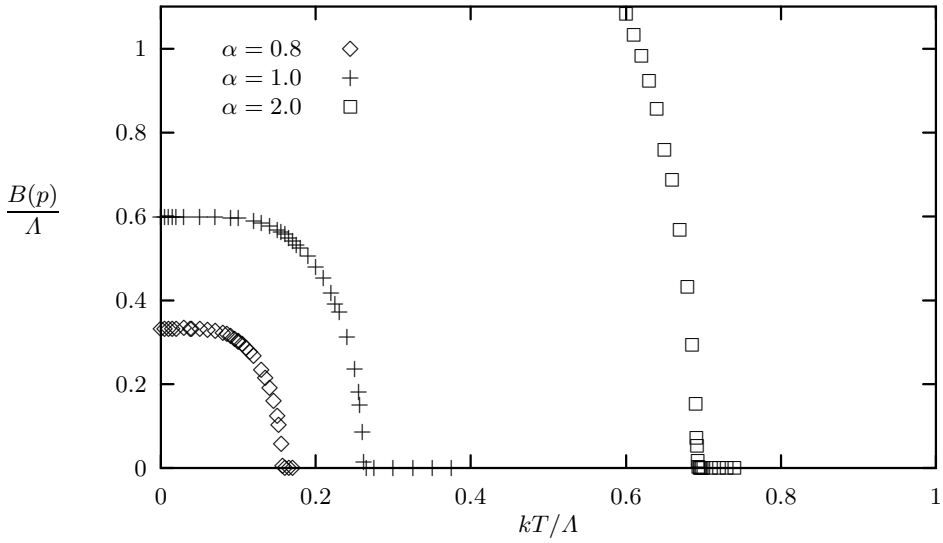

Fig. 6. Dynamical fermion mass as a function of temperature T for $Ng = 0$ at $p = 0.1\Lambda$.

If the thermal photon mass is included ($Ng = 1$), the essential feature of the behavior of the mass function is more or less the same as in the case without the thermal photon mass. The α and T dependences of the mass function $B(p)$ are presented in Figs. 7 and 8.

We recognize that the behavior of the mass function in the low temperature region, as seen in Figs. 6 and 8, is significantly different from that in the case without

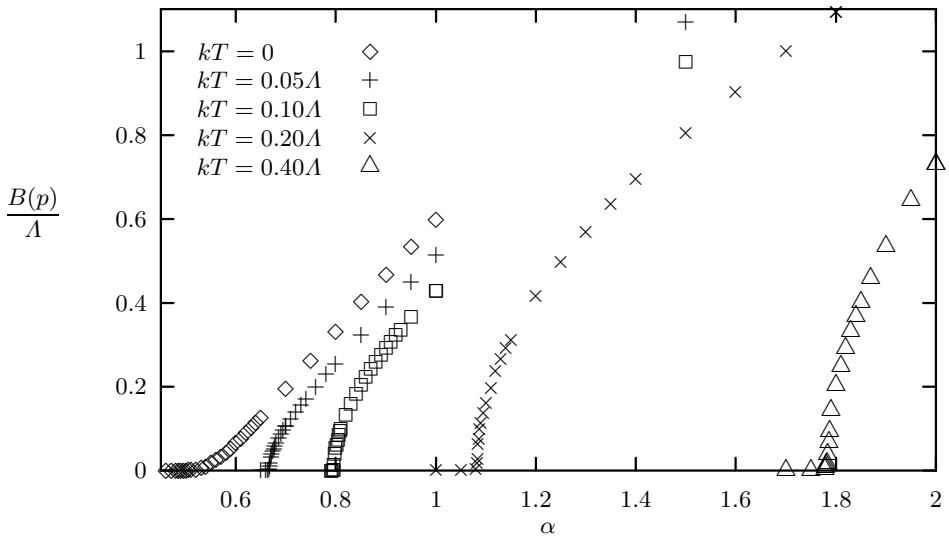

Fig. 7. Dynamical fermion mass as a function of the coupling constant α for $Ng = 1$ at $p = 0.1\Lambda$.

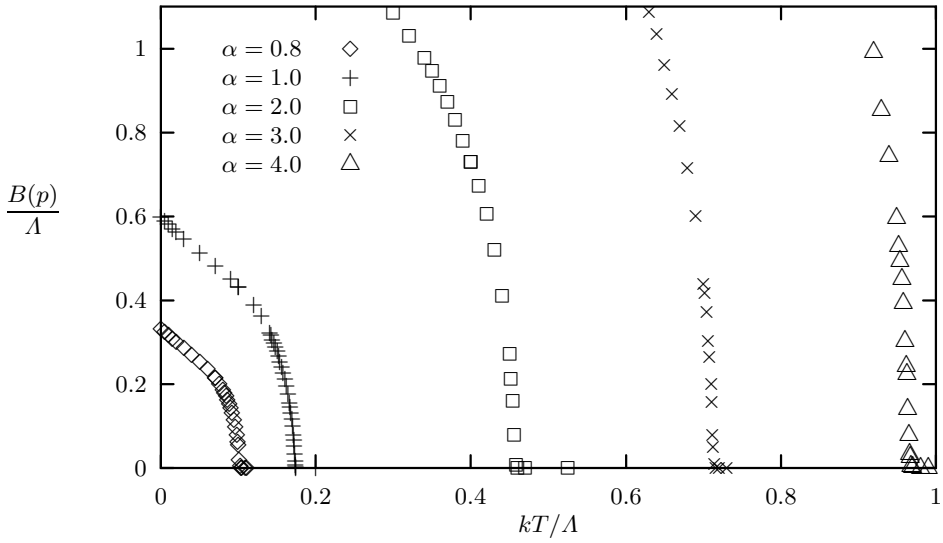

Fig. 8. Dynamical fermion mass as a function of the temperature T for $Ng = 1$ at $p = 0.1\Lambda$.

the thermal photon mass. Similar behavior is observed in the case $Ng = 3$, although the result is not shown in the figures.

§6. Critical curve and critical exponents

By considering the figures obtained in the last section, we can directly draw the critical curve in the T-α plane. In fact, for the case with $Ng = 0$, we pick out the values of α where the mass function vanishes and plot those values as a function of temperature. The resulting curve is the critical curve for the case $Ng = 0$. In order to perform this procedure in a more systematic way and to obtain critical exponents simultaneously, we apply the following method.

We fit the function $B(p)$ with n data points, B_i, α_i and T_i, with $i = 1, \cdots n$ near the critical point by assuming the functional form

$$B(p) = e^{C_T}(T_c - T)^{\nu} \tag{6·1}$$

for fixed coupling constant α, and

$$B(p) = e^{C_\alpha}(\alpha - \alpha_c)^{\eta} \tag{6·2}$$

for fixed temperature T. Here C_T, C_α, T_c, α_c, ν and η are adjustable parameters, with α_c and T_c corresponding to the critical coupling constant and critical temperature, and ν and η designate the critical exponent. To estimate the values of C_T, C_α, T_c, α_c, ν and η, we adopt the standard least-squares fit. We choose n data points near the critical point and minimize the quantities

$$\sum_{i=1}^{n}[\ln B_i - (\nu \ln(T_c - T_i) + C_T)]^2, \tag{6·3}$$

with coupling constant α fixed, and

$$\sum_{i=1}^{n}[\ln B_i - (\eta \ln(\alpha_i - \alpha_c) + C_\alpha)]^2, \tag{6·4}$$

with temperature T fixed.

The critical curves for $Ng = 0$, $Ng = 1$, $Ng = 3$ and $Ng = \infty$ are shown in Fig. 9. Taking the $N \to \infty$ limit in Eq. (3·16) we find that the dynamical fermion mass for $Ng = \infty$ is obtained by replacing α by $(2/3)\alpha$ in the case $Ng = 0$. Thus the critical coupling constant α_c for $Ng = \infty$ is given by that for $N = 0$ multiplied by 2/3, within our approximation. Note that our choice of the function puts no constraints on the number of fermion flavors, whereas in strong coupling QED at $T = 0$, there might be a critical value N_c above which there is a chiral symmetric phase only.[14] This may imply that terms which are independent of temperature in the vacuum polarization function Π also have a strong influence on the chiral phase transition. Therefore our approximation is not valid in the $N \to \infty$ limit. The longitudinal mode of the photon propagator acquires a non-vanishing thermal mass for $Ng \neq 0$. Since the thermal photon mass $m_{\rm ph}$ tends to suppress the gauge interaction, it has the effect of maintaining the chiral symmetry. As is seen in Fig. 9, the critical coupling α_c increases as the effect of the thermal photon mass is enhanced.

In Fig. 10, the critical exponents ν and η are shown as functions of the temperature and coupling constant, respectively. As is seen in Fig. 10, the critical exponents do not depend on the number of fermion flavors Ng. This guarantees the accuracy of our numerical analysis. The dependence on the coupling constant α is not clear in our numerical result. Taking the average of the critical exponents ν for $\alpha = 1, 2, 3$

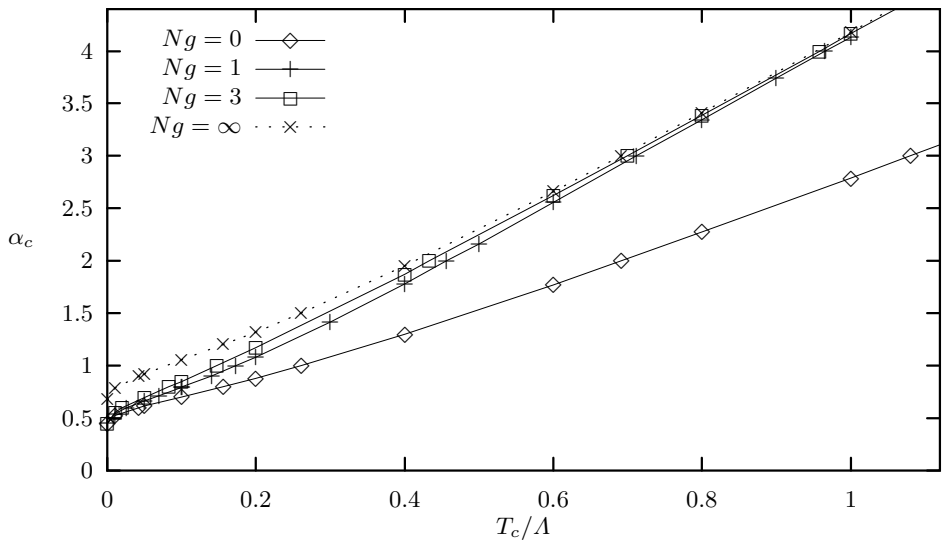

Fig. 9. Critical curves for $Ng = 0, Ng = 1, Ng = 3$ and $Ng = \infty$ at $p = 0.1\Lambda$.

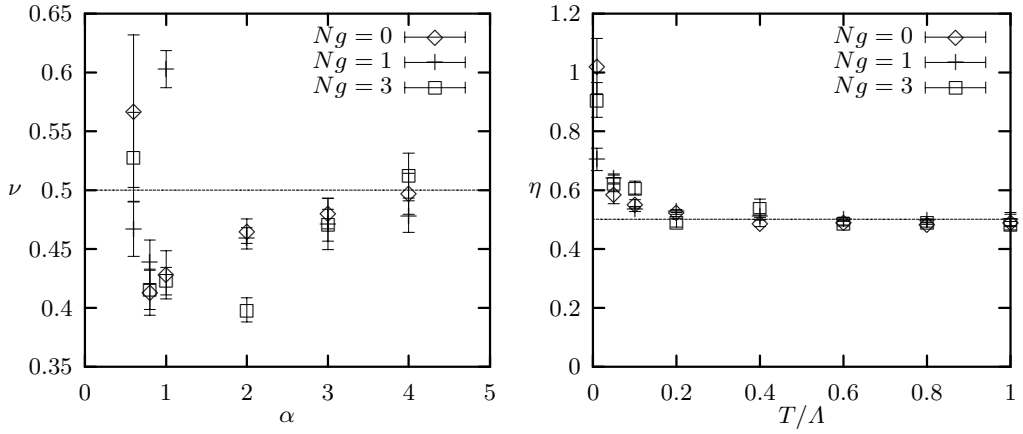

Fig. 10. Critical exponents ν and η evaluated at $p = 0.1\Lambda$.

and 4 and η for $T/\Lambda = 0.2$, 0.4, 0.6, 0.8 and 1.0, we obtain

$$\nu \sim \begin{cases} 0.46 & \text{for} \quad Ng = 0, \\ 0.50 & \text{for} \quad Ng = 1, \\ 0.45 & \text{for} \quad Ng = 3, \end{cases} \tag{6·5}$$

and

$$\eta \sim \begin{cases} 0.49 & \text{for} \quad Ng = 0, \\ 0.51 & \text{for} \quad Ng = 1, \\ 0.49 & \text{for} \quad Ng = 3, \end{cases} \tag{6·6}$$

respectively. Therefore our results are consistent with $\nu = 1/2$ and $\eta = 1/2$, which are in accordance with the critical exponents in the four-fermion theory.[13)]

In Fig. 11, the Ng dependence of the mass function is presented. Since the longitudinal mode for the photon propagator acquires a thermal mass for $Ng \neq 0$, the photon propagator has only one massless mode. On the other hand, the photon propagator has three massless modes for $Ng = 0$. As seen in Fig. 11, the dynamical fermion mass depends strongly on the number of massless modes in the photon propagator near the critical temperature, where the instantaneous exchange approximation is valid.

Note that the results for the behavior of the critical curve and the dynamical fermion mass for finite Ng seem different from those in Ref. 7). There, the thermal photon mass is introduced both for the longitudinal and transversal modes. In this case, there is no massless mode for the photon propagator. If we set the magnetic photon mass proportional to T^2, we obtain a result that is consistent with that in Ref. 7).

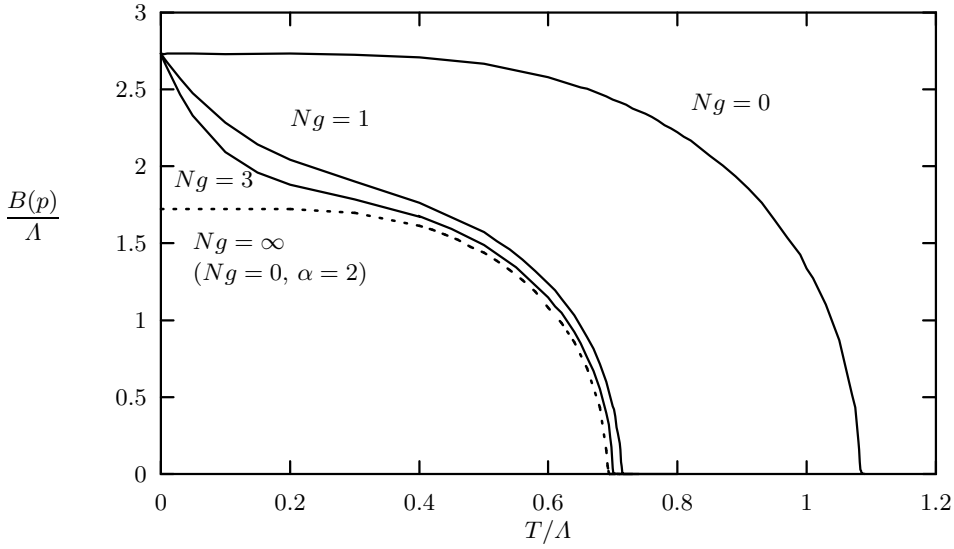

Fig. 11. Dynamical fermion mass for $Ng = 0$, $Ng = 1$, $Ng = 3$ and $Ng = \infty$ as a function of the temperature T at $\alpha = 3$ and $p = 0.1\Lambda$.

§7. Conclusion

We have investigated the mechanism of chiral symmetry breaking in strong-coupling Abelian gauge theories at finite temperature. The Schwinger-Dyson equation in the Landau gauge was solved numerically within the framework of the instantaneous exchange approximation, which is valid at high temperature. The effect of the thermal mass for the photon propagator on the phase transition was also clarified. The following are our results in order:

1. The fermion wave function effect is negligible in the high temperature region; i.e., $A_0 = A = 1$.
2. The chiral phase transition is found to be second order in the high temperature region. Thus, the physical mass obeys a scaling law of the mean-field type. The effect of the temperature on the chiral phase transition seems to be equivalent to the fermion loop effect in strong coupling QED at $T = 0$.
3. The critical temperature increases linearly as a function of the critical coupling constant in the high temperature region. This result contradicts that of Ref. 7), where it is claimed that the chiral symmetry is always restored at finite temperature, no matter how large the coupling constant becomes. The origin of this discrepancy lies in the vacuum polarization function. We have considered its transverse and longitudinal parts separately [see Eq. (3·1)], while in Ref. 7), they were assumed to be the same.
4. The thermal photon mass reduces the effect of electromagnetic interaction. It should be noted that the vertex correction coming from the hard thermal loop cannot be neglected if the external momentum is soft, i.e., $O(eT)$.

In the IE approximation, the imaginary part of the fermion wave function disappears. For this reason, the effect of the fermion damping is not included in our approach. This may have a strong influence on the phenomena at high temperature. To include this effect, we cannot use the IE approximation and consider the case with non-vanishing fermion wave functions. For this purpose it is necessary to analyze the Schwinger-Dyson equation beyond the ladder approximation.

The next improvement we should make is to extend our analysis to the low temperature region. To realize this, there are some difficulties to be overcome:

1. The vacuum polarization function at low temperature has to be estimated with some suitable approximation or using numerical calculations.
2. Proper approximations have to be determined in order to solve the Schwinger-Dyson equation at low temperature. Otherwise the equation is much too complicated.

We believe that the structure of the chiral phase transition is the same in general as in the case we have investigated. This will be the subject of a forthcoming paper.

Acknowledgements

The authors would like to thank S. D. Odintsov for useful conversations in the early stages of the present work and K.-I. Kondo for enlightening discussions. We also thank H. Nakkagawa, H. Yokota and Y. Fueki for useful discussions about the validity of our approximation. The present work was supported by Monbusho funds (Grant-in-Aid for Scientific Research (C) and Grant-in-Aid for Encouragement of Young Scientists, from the Ministry of Education, Science, Sports and Culture) with contract numbers 08640377 (T. M.), 11640280 (T. M.) and 11740154 (T. I.).

Appendix A

—— *Critical Coupling at Vanishing Temperature* ——

Here we calculate the critical value of the coupling constant α_c at vanishing temperature within the instantaneous exchange approximation, though this approximation is valid only at high temperature.

We begin with the linearized Schwinger-Dyson equation

$$B(p) = \frac{3\alpha}{4\pi p}\int_0^\Lambda dqB(q)\ln\frac{(p+q)^2}{(p-q)^2}, \tag{A·1}$$

which is taken from Eq. (3·16) by setting $T=0$ and neglecting the mass function in the denominator. If we take only the first term in the expansion of the logarithm,

$$\ln\frac{(p+q)^2}{(p-q)^2} = \sum_{n=0}^{\infty}\frac{4}{2n+1}\left[\left(\frac{q}{p}\right)^{2n+1}\theta(p-q)+\left(\frac{p}{q}\right)^{2n+1}\theta(q-p)\right], \tag{A·2}$$

it is easily found that the Schwinger-Dyson equation,

$$B(p) \simeq \frac{3\alpha}{\pi p}\int_0^\Lambda dqB(q)\left[\frac{q}{p}\theta(p-q)+\frac{p}{q}\theta(q-p)\right], \tag{A·3}$$

has the following nontrivial solution:

$$B(p) \propto p^{\lambda}\,, \qquad \lambda = \begin{cases} -1+\sqrt{1-\dfrac{6\alpha}{\pi}}, & \left(0<\alpha<\dfrac{\pi}{6}\right) \\ -1 \pm i\sqrt{\dfrac{6\alpha}{\pi}-1}. & \left(\alpha>\dfrac{\pi}{6}\right) \end{cases} \tag{A·4}$$

When the value of coupling constant α lies in the region $\alpha < \pi/6$, λ is real, and the system is in the symmetric phase. However, when the value of α lies in the region $\alpha > \pi/6$, λ is complex, so that the solution of the Schwinger-Dyson equation is an oscillatory function, and the system is in the broken phase.[3] The critical value α_c in this case is $\pi/6$, which is half of the well-known value $\pi/3$ in Landau gauge. This difference results from the instantaneous exchange approximation and the simplification of the logarithm.

The evaluation of the critical value in the case including the full term of Eq. (A·2) is made as follows. The Schwinger-Dyson equation (A·1) with the expansion Eq. (A·2) reads

$$\begin{aligned} B(p) = {} & \frac{3\alpha}{\pi p}\sum_{n=0}^{\infty}\frac{1}{2n+1} \\ & \times \int_0^{\Lambda} dq B(q)\left[\left(\frac{q}{p}\right)^{2n+1}\theta(p-q)+\left(\frac{p}{q}\right)^{2n+1}\theta(q-p)\right], \end{aligned} \tag{A·5}$$

and we take the solution of the form $B(p) \propto p^{\lambda}$, which is valid in the above simplified case. Note that the value of λ is restricted by the inequality $-2 < \mathrm{Re}\lambda < 0$, due to the condition that the integral in Eq. (A·5) is finite. Then the Schwinger-Dyson equation can be reduced to

$$\frac{3\alpha}{2(\lambda+1)}\tan\frac{\pi(\lambda+1)}{2} = 1, \tag{A·6}$$

by performing the integral and using the formula

$$\sum_{n=0}^{\infty}\frac{1}{(2n+1)^2-x^2} = \frac{\pi}{4x}\tan\frac{\pi x}{2}. \tag{A·7}$$

The real solution of Eq. (A·6) is easily found by considering the inclinations of $\tan\pi(\lambda+1)/2$ and $2(\lambda+1)/3$ at $\lambda=-1$. The result is that the nontrivial solution λ is real when $0<\alpha<4/(3\pi)$, which corresponds to the symmetric phase, whereas Eq. (A·6) has complex solutions when $\alpha > 4/(3\pi)$, which corresponds to the broken phase. Hence, the critical value of the coupling constant in this case is

$$\alpha_c = \frac{4}{3\pi}. \tag{A·8}$$

The exact value of critical coupling constant can be evaluated numerically, by fitting data with a function in the form of the Miransky scaling law, and we find that

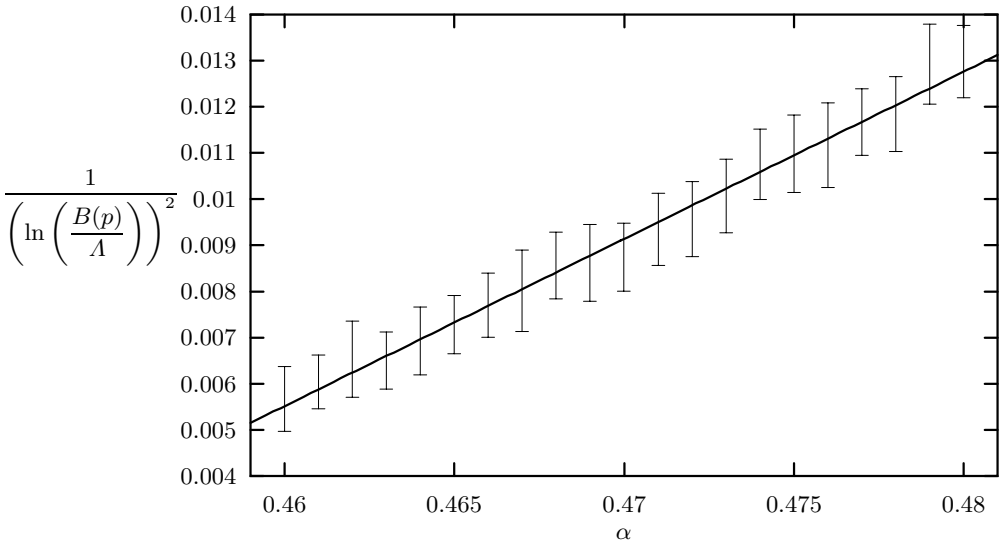

Fig. 12. $1/(\ln(B(p)/\Lambda))^2$ as a function of α with a fitted line. The critical value is given by $\alpha_c = 0.44477 \pm 0.00053$.

the result is $\alpha_c \approx 0.445$. There is a significant discrepancy between this numerical value and our theoretical prediction $4/(3\pi)$. It is easy to understand that this discrepancy is due to the fact that we made a linearization approximation. It should be pointed out here that the mass function in the denominator of Eq. (3·16) is ignored in Eq. (A·1). This implies that the exact value of α_c must be slightly larger than $4/(3\pi)$, and should be in the range

$$\frac{4}{3\pi} < \alpha_c \leq \frac{\pi}{6}. \tag{A·9}$$

The numerical value falls within this range.

References

1) M. Baker, K. Johnson and R. S. Willey, Phys. Rev. Lett. **11** (1963), 518; Phys. Rev. **136** (1964), B1111; **163** (1967), 1699.
2) T. Maskawa and H. Nakajima, Prog. Theor. Phys. **52** (1974), 1326; **54** (1975), 860.
3) R. Fukuda and T. Kugo, Nucl. Phys. **B117** (1976), 250.
4) See, e.g. V. A. Miransky, *Dynamical Symmetry Breaking in Quantum Field Theories* (World Scientific Pub. Co., 1993) for a full list of references.
5) F. J. Dyson, Phys. Rev. **75** (1949), 1736.
J. Schwinger, Proc. Natl. Acad. Sci. USA **37** (1951), 452, 455.
6) T. Akiba, Phys. Rev. **D36** (1987), 1905.
7) K.-I. Kondo and H. Yoshida, Int. J. Mod. Phys. **A10** (1995), 199.
8) G. Triantaphyllou, Phys. Rev. **D58** (1998), 065006.
9) H. Umezawa, H. Matsumoto and M. Tachiki, *Thermo Field Dynamics and Condensed States* (North-Holland Pub. Co., 1982).
10) J. I. Kapusta, *Finite Temperature Field Theory* (Cambridge University Press, 1989).
11) M. Le Bellac, *Thermal Field Theory* (Cambridge University Press, 1996).
12) A. Das, *Finite Temperature Field Theory* (World Scientific Pub. Co., 1997).
13) T. Inagaki, T. Kouno and T. Muta, Int. J. Mod. Phys. **A10** (1995), 2241.

14) K.-I. Kondo and H. Nakatani, Nucl. Phys. **B351** (1991), 236; Prog. Theor. Phys. **88** (1992), 737.